THE JOURNAL OF PHYSICAL CHEMISTRY A

Article

pubs.acs.org/JPCA

Which Density Functional Should Be Used to Describe Protonated Water Clusters?

Ruili Shi,[†] Xiaoming Huang,[‡] Yan Su,[*,†] Hai-Gang Lu,[§] Si-Dian Li,[§] Lingli Tang,[⊥] and Jijun Zhao[†]

[†]Key Laboratory of Materials Modification by Laser, Ion and Electron Beams, Dalian University of Technology, Ministry of Education, Dalian, 116024, China

[‡]School of Ocean Science and Technology, Dalian University of Technology, Panjin Campus, Panjin, 124221, China

[§]Key Laboratory of Chemical Biology and Molecular Engineering of the Education Ministry, Institute of Molecular Science, Shanxi University, Taiyuan, 030006, China

[⊥]College of Science, Dalian Nationalities University, Dalian 116600, China

Supporting Information

ABSTRACT: Protonated water cluster is one of the most important hydrogen-bond network systems. Finding an appropriate DFT method to study the properties of protonated water clusters can substantially improve the economy in computational resources without sacrificing the accuracy compared to high-level methods. Using high-level MP2 and CCSD(T) methods as well as experimental results as benchmark, we systematically examined the effect of seven exchange-correlation GGA functionals (with BLYP, B3LYP, X3LYP, PBE0, PBE1W, M05-2X, and B97-D parametrizations) in describing the geometric parameters, interaction energies, dipole moments, and vibrational properties of protonated water clusters $H^+(H_2O)_{2-9,12}$. The overall performance of all these functionals is acceptable, and each of them has its advantage in certain aspects. X3LYP is the best to describe the interaction energies, and PBE0 and M05-2X are also recommended to investigate interaction energies. PBE0 gives the best anharmonic frequencies, followed by PBE1W, B97-D and BLYP methods. PBE1W, B3LYP, B97-D, and X3LYP can yield better geometries. The capability of B97-D to distinguish the relative energies between isomers is the best among all the seven methods, followed by M05-2X and PBE0.

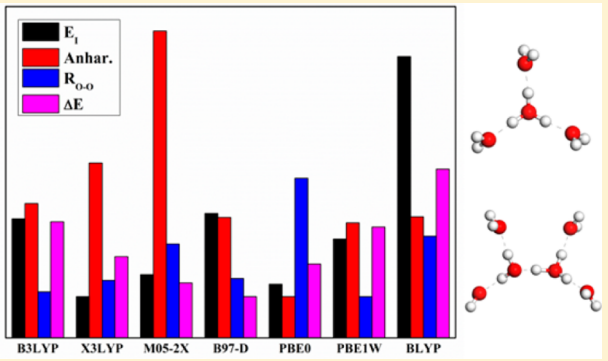

INTRODUCTION

Water is essential to all kinds of life forms.[1] Hence, both neutral water clusters and hydrated ion clusters have drawn great amount of attention.[2−13] When a neutral water cluster uptakes an extra proton (hydrogen) which forms strong covalent bond with one of the oxygen atoms, the neutral water cluster becomes a hydronium ion cluster, also known as protonated water cluster. Protonated water clusters widely exist in aqueous solution and play a very important role for many chemical and biological reactions. The study of protonated water clusters helps explain the formation of cloud, haze, and the proton transfer process related to many chemical or biological reactions in aqueous solution.[14−17] Since the fundamental chemical and physical properties of a cluster sensitively depend on cluster size, extensive experimental and theoretical efforts have been devoted to the structural, vibrational, and other properties of protonated water clusters as a function of cluster size.

Experimentally, small protonated water clusters have been investigated since 1960s. Good et al. obtained protonated water clusters by pulsing electron-beam high-pressure mass spectrometry.[18] For protonated water monomer, the extra proton forms strong covalent bond with one oxygen atom, namely the H_3O^+ Eigen ion,[19] having a trigonal pyramidal structure. Many subsequent experimental studies[20−22] have confirmed that H_3O^+ and more water molecules can form hydrogen-bonded complexes in the gas phase. For protonated water dimer, there are two configurations: one is the Zundel ion[23] with the extra hydrogen in the middle of the two oxygen atoms (C_2 symmetry); and another is the C_s symmetry of $H_3O^+{\cdot}H_2O$ cluster. The Zundel type has been demonstrated to be the ground state by many experiments.[24−32] For protonated water trimer, Yeh et al. used a tandem mass spectrometer and a radiofrequency ion trap to measure the gas phase infrared (IR) spectra from 3550 to 3800 cm^{-1}.[24] For $n \geq 4$, Jiang et al. conducted pioneering IR spectroscopic investigation of medium sized $H^+(H_2O)_n$ clusters with n = 5−8 in the gas phase via vibrational predissociation spectroscopy.[33] Headrick et al. reported how the vibrational spectra of protonated water clusters evolve due to local environment of the excess proton

Received: January 3, 2017
Revised: March 23, 2017
Published: April 6, 2017

DOI: 10.1021/acs.jpca.7b00058
J. Phys. Chem. A XXXX, XXX, XXX−XXX

through laser generation of infrared light in the 1000−4000 cm^{-1} range. It was found that the structures of the cluster ions could retain a chain like topology up to $n = 6$, while the single-ring isomer starts at $n = 7$.[34] While Miyazaki et al. demonstrated that $n = 10$ is the boundary of chain like structures and two-dimensional net structures through the IR spectroscopy of $H^+(H_2O)_{4-27}$.[6]

Theoretically, the structure, vibrational frequency, binding energy, dipole moment, isotope effect, and structural transition of protonated water clusters have been comprehensively investigated by various empirical potentials and ab initio methods. Kozack et al. developed empirical potentials for $H^+(H_2O)_n$ (proton model) and $H_3O^+(H_2O)_{n-1}$ (hydronium model) clusters ($n \leq 7$).[35] They found that while both models yield minimum-energy structures in good agreement with ab initio studies, the experimental hydration energies are much better accounted for within the proton model. Hodges and Stone developed an anisotropic site potential (ASP) to model the interaction between H_3O^+ and H_2O, which is able to search the low-energy structures on the potential energy surface (PES) of protonated water clusters, i.e., $H_3O^+(H_2O)_n$ clusters for n = 1−7.[36]

As the cluster size increases, the number of structural isomers increases dramatically. Abundant quantum chemical computations concentrated on searching the global minima of hydronium water clusters by comparing the isomer energies.[37−43] For example, Park et al. investigated the difference of structures and infrared spectra between Eigen and Zundel configurations using ab initio molecular dynamics (AIMD) simulations as well as high level ab initio calculations.[44] Using the scaled hypersphere search method on the Hartree−Fock PES, Luo et al. found 174 isomers for $H^+(H_2O)_8$ cluster, and then computed 168 isomers at the B3LYP/6-31+G** level.[40] They proposed that a cagelike structure with "Eigen" feature is the global minimum. Do and Besley used basin hopping (BH) algorithm combined with density functional theory (DFT) to search the equilibrium structures of protonated water clusters $H^+(H_2O)_n$ with $n \leq 9$.[43] They found a new global minimum for $H^+(H_2O)_7$ cluster that is 0.515 kcal/mol lower than that by Hodges and Wales[37] at B3LYP+D/6-31+G* level.

Spectral analysis can also reflect the structural characteristics of protonated water clusters.[45−50] Despite harmonic IR frequencies, anharmonic effect for protonated water clusters is also very important.[34] Torrent-Sucarrat and Anglada evaluated the anharmonic effect of IR frequencies of $H^+(H_2O)_{2-3,21}$ clusters at B3LYP/6-31+G(d)//B3LYP/6-311++G(3df,3pd) level and found that the anharmonic frequencies reproduced the experimental results well, meaning that the anharmonic effect is crucial for the vibrational properties of protonated water clusters.[51]

Clearly, comprehensive understanding of protonated water clusters calls for accurate description of hydrogen bonding in the molecular clusters, which remains a challenge for current DFT with general gradient approximation (GGA). There have been debates on the most appropriate functional for hydrogen bonding in water systems. For instance, Sprik et al. evaluated the performance of three gradient-corrected functionals (B, BP, and BLYP) for describing condensed aqueous systems and found BLYP could reproduce the experimental results well.[52] Using MP2 and coupled-cluster theory with singles, doubles, and perturbative triples excitations (CCSD(T)) results as benchmark, Li et al. examined the effect of 11 exchange-correlation functionals and basis sets on neutral $(H_2O)_n$ clusters up to $n = 10$, in which M05-2X/MG3S and X3LYP/6-31+G(2d,p) are the most appropriate combinations to depict geometries and energies of water clusters.[53] Plumley et al. tested the performance of nine functionals with 16 basis sets for the hydrogen bonded water dimer.[54] They suggested that the combinations of B3LYP, B97-D, M06, MPWB1K/D95(d,p), B3LYP/6-311++G(d,p), B3LYP, B97-D, MPWB1K/B95++(d,p), B3LYP, B97-D/6-311++G(d,p) and M05-2X, M06-2X, X3LYP/aug-cc-pVDZ are acceptable for hydrogen bonded systems. In addition, Liu et al. also assessed the performance of a variety of exchange−correlation functionals and various basis sets in describing the noncovalent interactions in the building clusters of methane hydrates.[55] B97-D, ωB97X-D, and M06-2X with 6-311++G(2d,2p) basis set without basis set superposition error (BSSE) correction were recommended for describing the noncovalent interactions in methane hydrate systems considering both accuracy and efficiency.

Despite the above efforts, there were only a few earlier works on evaluating the performance of DFT methods for protonated water clusters. A systematical examination of DFT methods for protonated water clusters is therefore crucial for comprehensively understanding their structures and properties. In this paper, we evaluated seven popular GGA functionals to model the structures, electronic properties, and relative energies of protonated water clusters $H^+(H_2O)_n$ with n = 2−9, 12 by using MP2, CCSD(T), or experimental results as benchmarks. Our results provide very useful information about the most appropriate functional to describe protonated water clusters, which is essential for study of larger clusters that are beyond the capability of high-level ab initio calculations.

METHODS

Ab initio calculations were performed using DFT, CCSD(T),[56−58] and MP2[59] methods implemented in Gaussian 09 program (hardware: Intel(R) Xeon(R) CPU E7−8857 v2 @ 3.00 GHz with 32 cores and 288 G memory).[60] Here, a variety of popular exchange-correlation functionals were examined, including the "pure" GGA functionals with BLYP,[61,62] PBE1W[63,64] and B97-D[65,66] parametrizations, the hybrid GGA functionals with PBE0,[67] B3LYP,[68] and X3LYP[69] parametrizations, and the dispersion-enhanced GGA with M05-2X parametrization.[70] B97-D is outstanding among most dispersion corrected methods (Table S1 in the Supporting Information). So B97-D is the only dispersion-correction functional used in this work. Table S2 in the Supporting Information shows the comparison of CPU time for CCSD(T), MP2, and seven DFT methods for the single-point-energy (SPE) calculation of 3I and 6I clusters. The time costs of DFT methods are all less than 1/10 of CCSD(T) and 3/4 of MP2 for both 3I and 6I clusters. Thus, it is necessary to find appropriate DFT methods to study protonated water clusters in view of the computational economy. Since the differences of average adjacent O−O distances of protonated water clusters between MP2/aug-cc-pVDZ and MP2/aug-cc-pVTZ results can be ignored (details are shown in Table S3 in the Supporting Information), all DFT and MP2 computations of the geometry optimization of $H^+(H_2O)_{2-9,12}$ clusters were done with the aug-cc-pVDZ basis set,[71,72] if there has no specific declaration. In this study, all the cluster configurations were fully optimized without any symmetry constraint. The Cartesian coordinates of all the isomer structures of $H^+(H_2O)_{2-9,12}$ clusters could be found in Table S6 of the Supporting Information.

DOI: 10.1021/acs.jpca.7b00058
J. Phys. Chem. A XXXX, XXX, XXX−XXX

The frequency calculations at the same level with geometry optimizations were performed to confirm that each optimized structure is a true minimum without imaginary vibration frequency as well as to obtain the zero-point-energy (ZPE). Further calculations of the SPE were performed with aug-cc-pVTZ basis set. Total energies at MP2/aug-cc-pVTZ//MP2/aug-cc-pVDZ+ZPE level of theory are used to rank the energy order of all the isomers. Meanwhile, BSSE is taken into account for all interaction energies in this work. BSSE correction (ΔE_{BSSE}) was calculated using the following definition based on the site−site function counterpoise method proposed by Wells and Wilson:[73]

$$\Delta E_{BSSE} = \sum_{i=1}^{m} [E^{full}(fragm) - E^{fragm}(fragm)] \quad (1)$$

where superscript "*full*" or "*fragm*" is the energy calculated in the full basis set or in the fragment basis set, and m is the number of fragments for a given cluster.

In order to get more accurate reference values, we extrapolate the interaction energies of $H^+(H_2O)_{2-9,12}$ to complete basis set (CBS) limit. We calculated the SPE of protonated water clusters using aug-cc-pVηZ (η = 2, 3, 4, 5, 6) basis set. Then the CBS limit for the Hartree−Fock energies were calculated with the extrapolation of Petersson et al.:[74]

$$E_{XY}(HF) = \frac{e^{-a\sqrt{Y}}E_X - e^{-a\sqrt{X}}E_Y}{e^{-a\sqrt{Y}} - e^{-a\sqrt{X}}} \quad (2)$$

Here X and Y are the η-level basis set with $X < Y$, and a = 6.3.[74] Meanwhile, the CBS limit for the correlation energies were extrapolated using the following equation:[75]

$$E_{XY}(corr) = \frac{X^3E_X(corr) - Y^3E_Y(corr)}{X^3 - Y^3} \quad (3)$$

The interaction energies of $H^+(H_2O)_{2-3}$ clusters calculated using CCSD(T) and MP2 methods with BSSE-correction are shown in Table S4 in the Supporting Information. CBSXY is the result extrapolated from aug-cc-pVηZ with $\eta = X$ and Y basis set. The extrapolated results of MP2 and CCSD(T) are nearly the same. The results of CBS34 limit and larger CBS limit are almost identical. Considering the computational cost, here we use the TQ-zeta extrapolation at MP2 level as reference values for larger protonated water clusters, which is referred as MP2/CBS thereafter.

We define the root-mean-square deviation (RMSD) of interaction energies, anharmonic frequencies, average adjacent O−O distances, and energy differences of seven DFT methods compared to MP2 or experimental results to judge the performance of seven DFT methods. The RMSD for a given cluster size n is

$$\mathrm{RMSD} = \sqrt{\frac{1}{m}\sum_{i=1}^{m}(X_i^{Method} - X_i^{Benchmark})^2} \quad (4)$$

where m is the number of metastable isomers at each cluster size or the number of vibrational modes for anharmonic frequencies. X is the interaction energies, anharmonic frequencies, average adjacent O−O distances, or energy differences.

RESULTS AND DISCUSSION

Protonated Water Dimer and Trimer. The protonated water dimer and trimer are important model systems as benchmark to evaluate different theoretical methods owing to the availability of highly accurate *ab initio* results for comparison. Figure 1 provides the fully MP2/aug-cc-pVDZ optimized geometries of protonated water dimer and trimer.

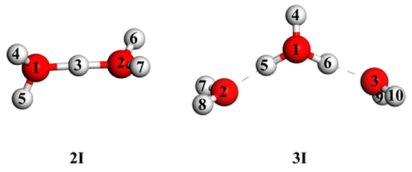

Figure 1. Equilibrium geometries of $H^+(H_2O)_{2-3}$ clusters. White and red balls denote hydrogen and oxygen atoms, respectively. The dashed lines represent hydrogen bonds.

We also employed more accurate CCSD(T) method to examine the reliability of MP2 results. The geometric parameters, dipole moments, and interaction energies of the protonated water dimer obtained at the CCSD(T), MP2, and DFT levels with aug-cc-pVQZ basis set are shown in Table 1. In order to remove differences caused by structure distortion predicted by different models, the dipole moments and interaction energies were obtained from SPE calculation using the same structure from CCSD(T)/aug-cc-pVQZ geometry optimization for all methods.

As shown in Figure 1, the protonated water dimer has the "Zundel" structure with C_2 symmetry, in which the added proton is equidistant from the two O atoms. This result agrees with previous DFT calculations by Mijoule et al.[76] and Wei et al.[77] In Table 1, the distance between two O atoms of the protonated water dimer R_{O-O} is 2.386 Å at CCSD(T)/aug-cc-pVQZ level, which is substantially shorter than the O−O distance in neutral water dimer (2.914 Å at CCSD(T)/TZ2P(f, d)+ level[78] and 2.976 Å in experiment[79]). In other words, the two water clusters become closer by the extra proton. The O−H and O−O distances from MP2 method are almost the same as the CCSD(T) results with difference only ∼0.001 Å. Meanwhile, almost all the GGA functionals overestimate the O−H and O−O distances except for PBE0, which deviates from MP2 and CCSD(T) results only by about 0.002 Å. From MP2 results, R^a_{O-H} (1.196 Å) is larger than the O−H distance (0.957 Å) in a free water molecule experimentally,[79] which means the extra proton tends to weaken the O−H bonds. The same conclusion can be obtained from the other methods.

The dipole moments reflect the electron density distribution and chemical bonds of protonated water clusters. In Table 1, MP2 and CCSD(T) methods yield entirely the same dipole moment (4.959 D) for protonated water dimer. MP2 gives better dipole moment than the seven DFT methods, meaning that MP2 is more outstanding for describing electron density distribution than the seven DFT methods.[80] All the DFT functionals considered here overestimate the dipole moment by 0.037 to 0.092 D. Among them, M05-2X yields a value (4.996 D) closest to the MP2 and CCSD(T) results, whereas BLYP has the largest deviation. Otherwise, hybrid GGA methods outperform pure GGA methods on the dipole moments of protonated water dimer.[80]

The interaction energy (E_I) is also a crucial quantity to measure the intermolecular hydrogen bond strength in a

DOI: 10.1021/acs.jpca.7b00058
J. Phys. Chem. A XXXX, XXX, XXX−XXX

Table 1. Geometric Parameters, Dipole Moments (μ), and Interaction Energies (E_I) of $H^+(H_2O)_2$ Computed Using CCSD(T), MP2, and Seven Different Exchange-Correlation Functionals with aug-cc-pVQZ Basis Set[a]

	CCSD(T)	MP2	B3LYP	X3LYP	M05-2X	B97-D	PBE0	PBE1W	BLYP
R^a_{O-H} (Å)[b]	1.195	1.196	1.202	1.201	1.200	1.211	1.196	1.213	1.216
R^b_{O-H} (Å)[c]	0.966	0.966	0.967	0.967	0.965	0.971	0.965	0.975	0.977
R_{O-O} (Å)	2.386	2.387	2.401	2.399	2.396	2.419	2.389	2.421	2.429
μ (debye)	4.959	4.959	5.025	5.022	4.996	5.050	5.016	5.048	5.051
E_I (kcal/mol)	51.56 (52.04)	51.80 (52.22)	51.97	52.52	53.56	51.66	54.09	51.69	49.90

[a]The interaction energies at CCSD(T)/CBS and MP2/CBS level are in parentheses. [b]$R^a_{O-H} = (r_{o1-H3} + r_{o2-H3})/2$ [c]$R^b_{O-H} = (r_{o1-H4} + r_{o1-H5} + r_{o2-H6} + r_{o2-H7})/4$

protonated water cluster. Here the interaction energy of a protonated water cluster $H^+(H_2O)_n$ is defined as

$$E_I(n) = |E_{total} - \sum_{i=1}^{n} E_i| \quad (5)$$

where E_{total} denotes the total energy of protonated water cluster, E_i ($i = 1-n$) represents the energy of monomers in the geometry as in the cluster. As shown in Table 1, the E_I of protonated water dimer is 52.22 kcal/mol at MP2/CBS level, which agrees reasonably well with the CCSD(T)/CBS result (52.04 kcal/mol). X3LYP, M05-2X, and PBE0 overestimate the E_I value. B3LYP, PBE1W, B97-D, and BLYP underestimate the interaction energy of protonated water dimer. Among the seven DFT methods, B3LYP yields closest to CCSD(T), PBE0 yields the largest E_I (54.09 kcal/mol), BLYP gives the lowest E_I (49.90 kcal/mol).

Furthermore, we used MP2/aug-cc-pVTZ method to explore the PES of protonated water dimer. Figure 2 presents the 1D potential energy profile of protonated water dimer. The PES was derived by moving the extra proton along the O−O axis with the two water molecules fixed. The potential energy profile was fitted to a 1D harmonic oscillator potential well. The energy levels of 1D harmonic oscillator come from the eigenvalues of the corresponding Schrödinger equation: $E_n = (n + 1/2)\hbar\omega$, which are E_0 = 548 cm^{-1}, E_1 = 1643 cm^{-1}, ... From them, the fundamental vibration frequency of the O−H$^+$−O asymmetric stretching mode is ω = 1095 cm^{-1}, slightly larger than the experimental frequency (990 cm^{-1}).[81] We also fitted the 1D PES of $H_5O_2^+$ at CCSD(T) and seven DFT with aug-cc-pVTZ basis set to the 1D harmonic oscillator model. The wave numbers of the O−H$^+$−O asymmetric stretching mode from harmonic oscillator approximation and simulated harmonic IR frequencies using aug-cc-pVTZ basis set are summarized in Table 2. For each GGA functional, the harmonic results of the O−H$^+$−O asymmetric stretching mode are about 200 cm^{-1} larger than the simulated harmonic IR frequencies since the PES scan of the central proton transfer is done with unrelaxed coordinates of the rest of atoms. For harmonic oscillator approximation, CCSD(T) yields the best agreement with experimental results, followed by MP2. Using MP2 values as benchmark, DFT methods give 111 to 331 cm^{-1} higher wave numbers in harmonic oscillator fitting and 100 to 311 cm^{-1} higher in simulated IR frequency. Among the seven functionals explored, PBE1W gives poorest performance about the wave numbers both in harmonic model and IR frequency.

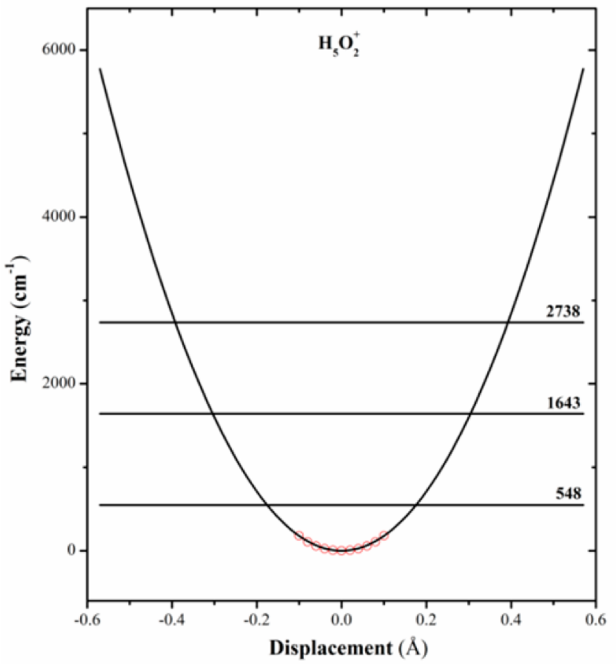

Figure 2. One-dimensional potential energy curve of $H_5O_2^+$ from harmonic oscillator fitting at MP2/aug-cc-pVTZ level. The red rings circles are the results from ab initio calculations.

Geometric parameters, dipole moments, and interaction energies of protonated water trimer from various methods are given in Table 3. The dipole moments and interaction energies were obtained from SPE calculation using the same structure from CCSD(T)/aug-cc-pVDZ geometry optimization for all methods. According to Table 3, O−O distances of all the seven GGA methods and MP2 are 0.002 Å to 0.053 Å lower than CCSD(T) value of 2.514 Å. Among them, BLYP (R_{O-O} is 2.512 Å) has best agreement with CCSD(T), followed by MP2 (2.504 Å), B97-D and PBE1W (2.500 Å). Taking CCSD(T) value of R^a_{O-H} as standard (1.014 Å), seven DFT functionals and MP2 overestimate this bond length by 0.001 Å to 0.019 Å. For R^b_{O-H}, MP2, B3LYP, X3LYP, M05-2X, and PBE0 underestimate it, while the other three methods overestimate it, as compared to CCSD(T). Basically, MP2 can reproduce the R^a_{O-H} and R^b_{O-H} of CCSD(T) results well. Among the seven DFT methods, BLYP describes these two kinds of O−H distances worst.

As shown in Table 3, MP2 reproduces the dipole moment of CCSD(T). Taking CCSD(T) value (1.953 D) as benchmark, the seven DFT methods tend to underestimate the dipole moment of protonated water trimer, which is opposite to the situation of protonated water dimer. Among them, M05-2X yields relatively close dipole moments of 1.893 D. PBE1W provides the worst dipole moment (1.766 D) of protonated water trimer. Hybrid GGA methods give better dipole moments than pure GGA methods.[80]

DOI: 10.1021/acs.jpca.7b00058
J. Phys. Chem. A XXXX, XXX, XXX−XXX

Table 2. Wavenumbers (in Units of cm^{-1}) of the O−H^+−O Asymmetric Stretching Mode from MP2 and Seven DFT Calculations with an aug-cc-pVTZ Basis Set

	CCSD(T)	MP2	B3LYP	X3LYP	M05-2X	B97-D	PBE0	PBE1W	BLYP
harmonic	1014	1095	1218	1206	1225	1320	1237	1426	1402
IR		910	1037	1025	1010	1125	1059	1221	1199

Table 3. Geometric Parameters, Dipole Moments (μ), and Interaction Energies (E_I) of $H^+(H_2O)_3$ Computed Using CCSD(T), MP2, and Seven Different Exchange-Correlation Functionals with aug-cc-pVQZ Basis Set Based on aug-cc-pVDZ Geometry[a]

	CCSD(T)	MP2	B3LYP	X3LYP	M05-2X	B97-D	PBE0	PBE1W	BLYP
R^a_{O-H} (Å)[b]	1.014	1.015	1.018	1.018	1.023	1.029	1.018	1.033	1.033
R^b_{O-H} (Å)[c]	0.969	0.968	0.967	0.966	0.963	0.970	0.964	0.975	0.977
R_{O-O} (Å)	2.514	2.504	2.493	2.489	2.461	2.500	2.474	2.500	2.512
μ (debye)	1.953	1.953	1.825	1.830	1.893	1.768	1.829	1.766	1.769
E_I (kcal/mol)	60.53 (61.04)	60.24 (60.82)	61.02	62.01	62.81	60.76	63.06	61.14	59.08

[a]The interaction energies at CCSD(T)/CBS and MP2/CBS level are in parentheses. [b]$R^a_{O-H} = (r_{o1-H4}+r_{o1-H5}+r_{o1-H6})/3$ [c]$R^b_{O-H} = (r_{o2-H7}+r_{o2-H8}+r_{o3-H9}+r_{o3-H10})/4$

According to Table 3, the interaction energy obtained from MP2/CBS (60.82 kcal/mol) is rather close to the CCSD(T)/CBS result (61.04 kcal/mol). Almost all the seven functionals overestimate the E_I value of CCSD(T), except for BLYP and B97-D. PBE0 yields the largest interaction energy (63.06 kcal/mol), BLYP gives the lowest E_I (59.08 kcal/mol). B97-D gives the best dipole moment compared to CCSD(T) result.

In this section, we demonstrate that MP2 can reproduce the CCSD(T) results for the geometric parameters, dipole moments, interaction energies, and vibrational frequencies of small protonated water clusters rather well. As a trade-off of the accuracy and computational cost, we use MP2 or experimental results as benchmark to evaluate the performance of the seven DFT methods to describe larger protonated water clusters in the following discussion.

Structures of $H^+(H_2O)_n$ (n = 2−9, 12) Isomers. Starting from the $H^+(H_2O)_n$ clusters with $n \geq 4$, there exist several isomers for each cluster size. All isomers and their relative energies for $H^+(H_2O)_n$ with n = 4−6 are shown in Figure 3, and those of $H^+(H_2O)_{7-9,12}$ are shown in Figure 4, Figure 5, Figure 6, and Figure 7, respectively. For a $H^+(H_2O)_n$ cluster, we rank the isomers based on the SPE calculation at MP2/aug-cc-pVTZ//MP2/aug-cc-pVDZ+ZPE level of theory and then

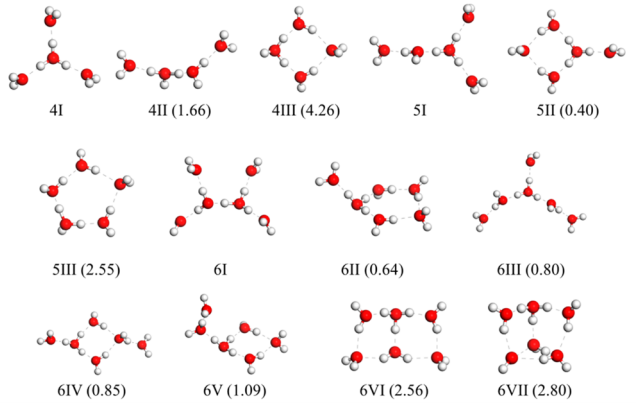

Figure 3. Structures of isomers for $H^+(H_2O)_{4-6}$ clusters. White and red balls denote hydrogen and oxygen atoms, respectively. The dashed lines represent hydrogen bonds. Relative energies resulting from SPE calculation at MP2/aug-cc-pVTZ level//MP2/aug-cc-pVDZ+ZPE level of theory are shown in parentheses (in units of kcal/mol).

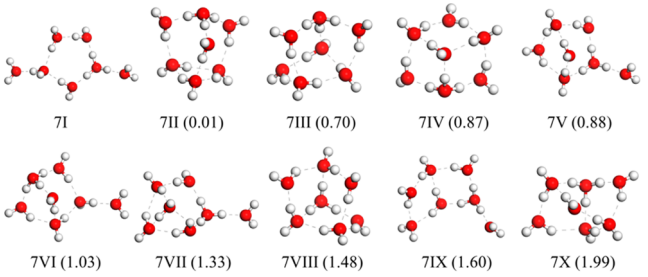

Figure 4. Structures of isomers for $H^+(H_2O)_7$ clusters. White and red balls denote hydrogen and oxygen atoms, respectively. The dashed lines represent hydrogen bonds. Relative energies resulting from SPE calculation at MP2/aug-cc-pVTZ//MP2/aug-cc-pVDZ+ZPE level of theory are shown in parentheses (in units of kcal/mol).

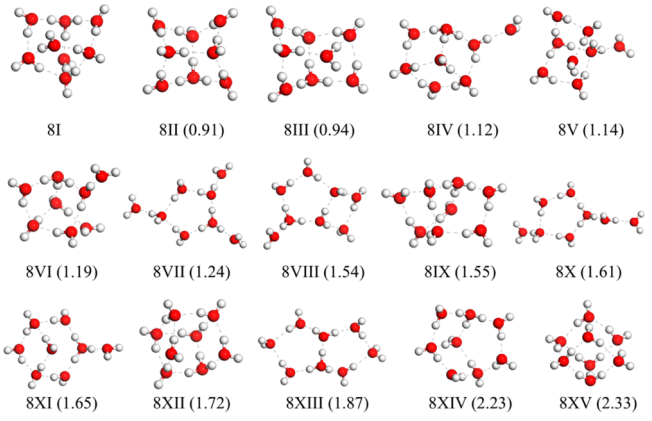

Figure 5. Structures of isomers for $H^+(H_2O)_8$ clusters. White and red balls denote hydrogen and oxygen atoms, respectively. The dashed lines represent hydrogen bonds. Relative energies resulting from SPE calculation at MP2/aug-cc-pVTZ//MP2/aug-cc-pVDZ+ZPE level of theory are shown in parentheses (in units of kcal/mol).

mark the ground state configuration as "nI" while the metastable isomers are ranked as "nII", "nIII", and so on. Most of the starting geometries are taken from the previous studies: 4II, 4III, 5II, 6III, 6VI, 6VII, 7III, and 8XV from Hodges et al.;[36] 5III, 6I, 6IV, and 6V from Kuo et al.;[38] 9II, 9III, 9VI, and 9XIV from Bankura et al.;[42] 7II, 7IV-7X, 8II-8V, 8VII, 8IX, 8X, 8XII, 8XV, 9VII, and 9IV, 9V, 9VIII, 9IX-9XIII from Nguyen et al.[41] The rest of the structures are obtained from

DOI: 10.1021/acs.jpca.7b00058
J. Phys. Chem. A XXXX, XXX, XXX−XXX

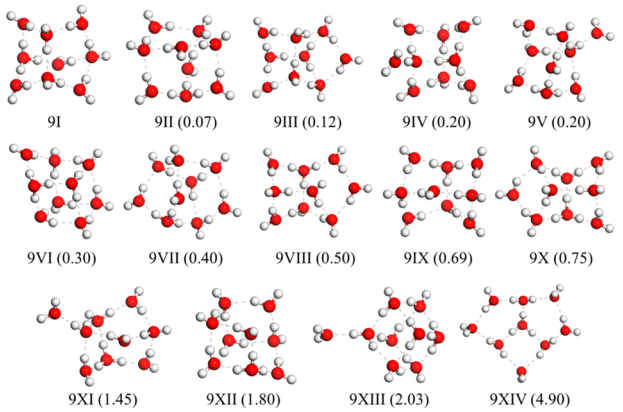

Figure 6. Structures of isomers for $H^+(H_2O)_9$ clusters. White and red balls denote hydrogen and oxygen atoms, respectively. The dashed lines represent hydrogen bonds. Relative energies resulting from SPE calculation at MP2/aug-cc-pVTZ//MP2/aug-cc-pVDZ level of theory are shown in parentheses (in units of kcal/mol).

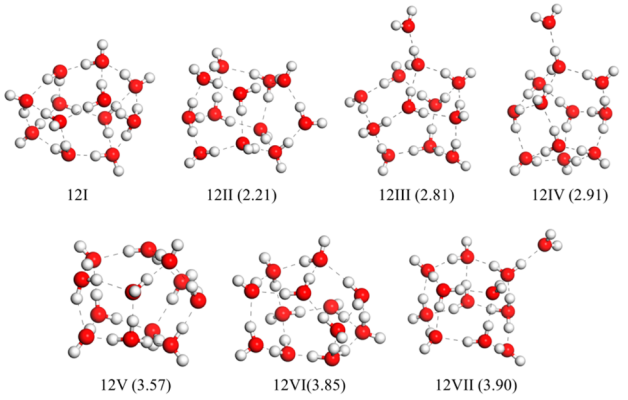

Figure 7. Structures of isomers for $H^+(H_2O)_{12}$ clusters. White and red balls denote hydrogen and oxygen atoms, respectively. The dashed lines represent hydrogen bonds. Relative energies resulting from SPE calculation at MP2/aug-cc-pVTZ//MP2/aug-cc-pVDZ level of theory are shown in parentheses (in units of kcal/mol).

global searched using the comprehensive genetic algorithm (CGA) developed by our own group,[82] in which the potential energy surface is described by the BLYP functional combined with double numerical plus *d*-functions (DND) basis set.

From our computations, MP2 and most DFT methods predict the same ground state structures for every cluster size, that is, a central H_3O^+ unit with two terminal water molecules for $H^+(H_2O)_3$, an open structure like Eigen ion for $H^+(H_2O)_4$, a chain like structure with an extra water molecule bonding to one of the outside water molecules of the ground state structure of $H^+(H_2O)_4$ for $H^+(H_2O)_5$, a H^+-centered chain like isomer for $H^+(H_2O)_6$, a five-member ring with two water molecules on two segregative knots for $H^+(H_2O)_7$, the bottom with a four-membered ring with one water molecule added to the second stable structure of $H^+(H_2O)_7$ for $H^+(H_2O)_8$, a three-dimensional structure with seven dangling hydrogens from seven water molecules for $H^+(H_2O)_9$, a monocage configuration with four pentagon-rings and four four-member rings for $H^+(H_2O)_{12}$. Moreover, M05-2X computation predicts the ground state structure for $H^+(H_2O)_6$ is 6II (a five-membered ring with a terminal water molecule on the H_3O^+ unit), and the lowest-energy structure for $H^+(H_2O)_7$ is 7II with an added H_3O^+ ion on top of one triangular prism composed of six water molecules. BLYP predicts that 8X is the most stable structure for $H^+(H_2O)_8$, which is the same with B3LYP. The ground state structure of $H^+(H_2O)_{12}$ is 12III with an extra water molecule added to a monocage according to the results of B3LYP, PBE1W, and BLYP calculations. The present results generally agree with previous work.[33,35−37,43,83]

Lowest-Energy Structures of $H^+(H_2O)_{2-9,12}$. Average adjacent O−O distance $\bar{R}_{o\text{-}o}$ can roughly characterize the structural properties of a protonated water cluster. Figure 8 shows the average adjacent O−O distance curve of lowest-energy structures of protonated water clusters with n = 2−9. For the size of n = 2−8 clusters with most ground state structures are quasi-planar ones, $\bar{R}_{o\text{-}o}$ increases as cluster size increases since the added proton weakens the intermolecular interactions. This trend is opposite to the case of neutral water clusters.[53] Both MP2 and DFT computations predict an increasing of O−O distances by ∼0.3 Å from dimer to $H^+(H_2O)_8$. Notably, for $H^+(H_2O)_9$, the $\bar{R}_{o\text{-}o}$ distance is slightly shorter than $H^+(H_2O)_8$ clusters (by about 0.012 Å) at MP2 and DFT (except for M05-2X) calculations. At each size, the average adjacent O−O distance of protonated water clusters is shorter than that of neutral water clusters,[53] and as the size increasing, the differences of average adjacent O−O distance between protonated water clusters and neutral water clusters become smaller.

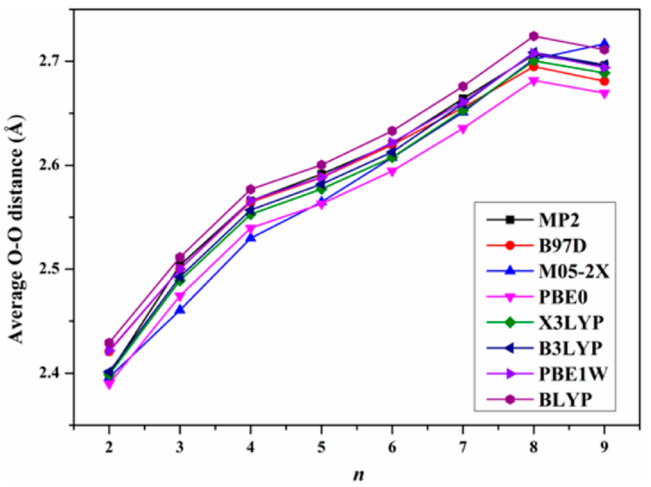

Figure 8. Schematic diagram of average adjacent O−O distance as a function of cluster size of the lowest-energy structures of $H^+(H_2O)_n$ clusters with n = 2−9 using MP2 method and seven different exchange-correlation functionals with the aug-cc-pVDZ basis set.

For average adjacent O−O distance, the RMSD of PBE1W, B3LYP, B97-D, X3LYP, BLYP, M05-2X, and PBE0 with regard to MP2 results are 0.005, 0.006, 0.008, 0.010, 0.014, 0.020, and 0.025 Å, respectively. Taking MP2 results as benchmark, the PBE1W results are best among all the functionals examined, followed by B3LYP. The performances of B97-D and X3LYP are also reasonably good. The other functionals can reproduce the size-dependent trend of $\bar{R}_{o\text{-}o}$ well, and their deviations to the MP2 values are all less than 1%. For example, PBE0, which is the worst case, only deviates from the MP2 results by 0.96% on average.

Table 4 summarizes the geometric parameters, interaction energies, dipole moments, and the number of hydrogen bonds of the lowest-energy structures of protonated water clusters.

DOI: 10.1021/acs.jpca.7b00058
J. Phys. Chem. A XXXX, XXX, XXX−XXX

Table 4. Geometric Parameters, Interaction Energies (E_I), Dipole Moments (μ), and the Number of Hydrogen Bonds (N_{HB}) for the Lowest-Energy Structures of $H^+(H_2O)_n$ (n = 2−9, 12) Computed Using MP2/aug-cc-pVTZ after Geometry Optimization at the MP2/aug-cc-pVDZ Level

n	$\bar{R}$o-o (Å)	E_I (kcal/mol)	E_I[a] (kcal/mol)	μ (debye)	N_{HB}
2	2.399	51.17	52.22	1.49	0
3	2.504	59.76	61.04	1.96	2
4	2.566	77.76	79.41	0.68	3
5	2.592	92.14	94.28	1.07	4
6	2.621	130.95	133.90	0.64	5
7	2.664	118.35	121.63	1.26	7
8	2.706	133.41	137.55	1.81	10
9	2.696	145.39	150.08	1.61	11
12	2.741	187.07	194.12	1.86	18

[a]The interaction energies are the results at MP2/CBS level.

The O−O distance of $H^+(H_2O)_2$ is 2.399 Å at MP2/aug-cc-pVDZ level, which is just 0.001 Å shorter than 2.40 Å at CCSD(T)/aug-cc-pVDZ level.[44] For $H^+(H_2O)_4$, the average adjacent O−O distance is 2.566 Å at MP2/aug-cc-pVDZ level, decreasing by 0.014 Å compared to CCSD(T)/aug-cc-pVDZ result.[44] The number of hydrogen bonds becomes larger as the cluster size increases.

According to Table 1 and Table 3, the MP2/CBS method can reproduce CCSD(T)/CBS results of protonated water dimer and trimer well. Therefore, we use MP2/CBS data as benchmark to evaluate the capacity of seven exchange-correlation functionals for describing interaction energies of protonated water clusters. The RMSD of interaction energies for the lowest-energy structures of $H^+(H_2O)_{2-9,12}$ at seven GGA methods with aug-cc-pVTZ basis set compared to those at MP2/CBS level are summarized in Table 5. It is obvious that X3LYP shows the best ability to describe E_I of protonated water clusters, followed by PBE0 and M05-2X. For small $H^+(H_2O)_n$ with up to n = 4, B97-D, PBE1W, and B3LYP outperform the interaction energies. The highlighted numbers in bold in Table 5 represent the maximum deviations for each method. One can see that BLYP gives the largest maximum deviation from MP2 results.

The harmonic and anharmonic frequencies of $H^+(H_2O)_{2-6}$ clusters calculated using MP2/aug-cc-pVDZ are shown in Table S5 of the Supporting Information. From Table S5 we can see that anharmonic frequencies are much closer to the experimental results. By comparing to the experimental frequencies of $H^+(H_2O)_{2-6}$ clusters,[24,34] we examine the performance of MP2 and seven DFT methods. The RMSD of the anharmonic frequencies of MP2 and seven DFT methods for the lowest-energy structures of $H^+(H_2O)_{2-6}$ are summarized in Table 6. First of all, MP2 method is outstanding for predicting the anharmonic frequencies of protonated water clusters. Among seven DFT methods, PBE0 gives the best results (average RMSD: 68 cm^{-1}), which is comparable to MP2 method (average RMSD: 67 cm^{-1}). PBE1W, B97-D, and BLYP yield acceptable anharmonic vibrational frequencies, followed by B3LYP and X3LYP methods. M05-2X provides the worst results, which deviate 507 cm^{-1} from the experimental values in average. Therefore, we recommend the PBE0 functional as an alternative to more costly MP2 method to simulate the anharmonic IR frequencies of protonated water clusters.

Structure and Energy Differences of $H^+(H_2O)_n$ (n = 4−9, 12) Isomers. Considering the existence of a large number of locally stable isomers with very small energy differences on the PES, a comprehensive study of the structure isomers of protonated water clusters with n = 4−9, 12 has been performed here. It is crucial to examine the performance of different DFT methods in distinguishing the isomers, which can be characterized by the differences of key geometric parameters and energy differences between the lowest-energy structure and the metastable isomers.

Table 7 summarizes the RMSD of average adjacent O−O distances $\bar{R}_{o\text{-}o}$ of seven DFT compared to MP2 methods at aug-cc-pVDZ level for $H^+(H_2O)_{4-9}$ isomers. Except for PBE0, all the DFT methods considered here give satisfactory geometrical properties for each cluster size. From the overall deviation of each functional using MP2 methods as benchmark, PBE1W yields the best structural parameters, with a RMSD of 0.0068 Å. B3LYP gives the second best overall performance with RMSD only 0.0008 Å higher than PBE1W. X3LYP and B97-D (RMSD are 0.0095 and 0.0098 Å, respectively) are also recommended to describe the geometrical properties of protonated water clusters, while M05-2X exhibits larger deviations from MP2 data. For a specific functional, its performance varies with cluster size. For example, B97-D gives very close geometries to MP2 results when n = 4−7. The highlighted results in bold in Table 7 represent the maximum deviations and PBE0 is worth being emphasized for 0.0329 Å. This functional gives the worst description for geometries of hydrogen-bonded systems. A similar conclusion was drawn by Li et al.[53] in previous benchmark calculations.

The RMSD of isomer energy differences for each functional could characterize the capability of each DFT method to distinguish the isomer energies, in which the effect of change of

Table 5. RMSD of the Lowest-Energy Structures for $H^+(H_2O)_{2\text{-}9,12}$ Interaction Energies of Seven Functionals with aug-cc-pVTZ Basis Set Compared to Those at the MP2/CBS Level (in Units of kcal/mol)

n	B3LYP	X3LYP	M05-2X	B97-D	PBE0	PBE1W	BLYP
2	0.58	1.13	2.20	0.26	**2.71**	0.32	1.49
3	0.36	1.36	2.19	0.03	2.45	0.45	1.65
4	0.73	0.73	1.30	1.44	1.82	0.67	3.43
5	1.32	0.61	1.66	2.32	2.02	1.19	4.83
6	3.15	0.70	1.49	5.12	2.06	3.90	9.18
7	3.21	0.01	1.94	4.12	1.99	2.55	8.55
8	5.89	1.46	1.89	5.58	0.80	4.56	12.65
9	6.50	1.49	1.83	6.28	1.19	4.87	14.15
12	**11.79**	**4.10**	**3.33**	**9.97**	**0.10**	**9.36**	**23.45**
average	3.73	1.29	1.98	3.90	1.68	3.10	8.82

DOI: 10.1021/acs.jpca.7b00058
J. Phys. Chem. A XXXX, XXX, XXX−XXX

Table 6. RMSD of the Anharmonic Frequencies of MP2 and Seven DFT Methods Compared to Experimental Results for the Lowest-Energy Structures of $H^+(H_2O)_{2-6}$ Clusters at aug-cc-pVDZ level (in Units of cm^{-1})

n	MP2	B3LYP	X3LYP	M05-2X	B97-D	PBE0	PBE1W	BLYP
2	61	57	48	312	151	6	166	201
3	54	68	478	266	**248**	86	142	179
4	28	36	21	**858**	178	56	198	176
5	85	103	96	343	197	**136**	**257**	**237**
6	**109**	**846**	**801**	756	222	54	187	209
average	67	222	289	507	199	68	190	200

Table 7. RMSD of Average Adjacent O−O Distances of Seven Functionals Compared to MP2 Geometries for Different Isomers of $H^+(H_2O)_n$ with n = 4−9, 12 Clusters at the aug-cc-pVDZ Level (in Units of Å)

n	B3LYP	X3LYP	M05-2X	B97-D	PBE0	PBE1W	BLYP
4	0.0069	0.0113	**0.0261**	0.0014	0.0254	0.0026	0.0137
5	0.0061	0.0116	0.0192	0.0040	0.0263	0.0040	0.0122
6	0.0077	0.0101	0.0145	0.0105	0.0248	0.0066	0.0163
7	0.0034	0.0071	0.0109	0.0089	0.0253	0.0075	0.0184
8	**0.0132**	**0.0175**	**0.0125**	**0.0183**	**0.0329**	**0.0134**	0.0177
9	0.0106	0.0055	0.0201	0.0116	0.0248	0.0115	0.0191
12	0.0054	0.0037	0.0054	0.0139	0.0253	0.0023	**0.0202**
average	0.0076	0.0095	0.0155	0.0098	0.0264	0.0068	0.0168

isomer rank order has already been reflected. For example, BLYP deviates most from the MP2 result as it has the largest change of isomer rank order for n = 6. The RMSD of isomer energy differences for each functional are summarized in Table 8. Like geometrical properties, the performance of isomer energy for a given functional is precarious. According to overall deviation of each functional, among all the functionals studied, B97-D performs best for describing the relative energies of protonated water clusters, giving an average deviation of 0.39 kcal/mol from the MP2 reference. M05-2X gives the second best performance (with average RMSD value of 0.52 kcal/mol), followed by PBE0 and X3LYP (with average RMSD values of 0.70 and 0.77 kcal/mol, respectively). BLYP gives the worst performance. With the cluster size increasing, BLYP and B3LYP methods give worse energy description compared to MP2. The maximum deviations for each DFT method are highlighted in bold in Table 8. As shown in Table 8, BLYP gives the largest maximum deviation (2.93 kcal/mol) among the seven DFT methods.

Table 8. RMSD of Isomer Energy Differences with ZPE-Correction of $H^+(H_2O)_n$ with n = 4−9, 12 for Seven Functionals Compared to Those at the MP2 Level with aug-cc-pVTZ Basis Set (in Units of kcal/mol)

n	B3LYP	X3LYP	M05-2X	B97-D	PBE0	PBE1W	BLYP
4	0.71	0.51	0.63	0.26	0.96	0.85	0.83
5	0.65	0.34	0.42	0.15	0.28	0.39	1.22
6	1.02	0.64	**0.86**	0.27	0.49	1.04	1.82
7	**1.95**	**1.41**	**0.53**	**0.69**	**1.12**	**2.06**	**2.93**
8	1.08	0.78	0.58	0.34	0.55	1.05	1.54
9	1.28	1.11	0.40	0.48	0.98	1.31	1.64
12	0.99	0.63	0.23	0.56	0.50	0.67	1.22
average	1.10	0.77	0.52	0.39	0.70	1.05	1.60

From the discussion in this subsection, we can draw the following conclusion: among the three pure GGA functionals, B97-D is distinguished in describing both geometric properties and relative energy of protonated water clusters, PBE1W is recommended to evaluate the geometry of $H^+(H_2O)_n$, while BLYP gives poor performance both in describing geometry and energy; among the three hybrid GGA methods, X3LYP is reliable to search the geometry and energy; B3LYP yields good results on structural computations, PBE0 is comparable to X3LYP for distinguishing the energy differences of $H^+(H_2O)_n$.

CONCLUSION

In this work, we investigated the interaction energies, anharmonic IR frequencies, geometry and energy differences of $H^+(H_2O)_n$ with n = 2−9, 12 to evaluate the performance of seven density functionals (B3LYP, X3LYP, M05-2X, B97-D, PBE0, PBE1W, and BLYP) by using MP2 method and experimental results as benchmark. First, we assessed the performance of MP2 compared to CCSD(T) by searching the geometry, electronic and vibrational properties of protonated water dimer and trimer. The results demonstrated that MP2 as benchmark is reliable to evaluate the ability of seven functionals to describe protonated water clusters. We then calculated the geometric parameters, interaction energies, dipole moments, anharmonic IR frequencies, and the number of hydrogen bonds of lowest-energy structures of $H^+(H_2O)_{2-9,12}$ clusters to verify that the aug-cc-pVDZ basis set for geometry optimization and aug-cc-pVTZ basis set for energy are adequate for this work. Generally speaking, the performance of GGA is acceptable for depicting protonated water clusters, while the overall performance of hybrid GGA is typically better than the nonhybrid ones. Among the seven GGA functionals, X3LYP is the best to describe the interaction energies. PBE0 is comparable to MP2 method for describing the anharmonic frequencies, which reproducing the experimental IR frequencies well. For geometrical properties, PBE1W, B3LYP, X3LYP, and B97-D are outstanding. PBE0 is not recommended to study the geometrical properties of $H^+(H_2O)_n$ clusters. B97-D yields best to distinguish the protonated water clusters isomers' energy differences. The performance of BLYP is not satisfactory. Definitely, our results provide a useful guidance in selecting the computational method that is most appropriate for studying protonated water clusters of large size.

DOI: 10.1021/acs.jpca.7b00058
J. Phys. Chem. A XXXX, XXX, XXX−XXX

■ ASSOCIATED CONTENT

Supporting Information

The Supporting Information is available free of charge on the ACS Publications website at DOI: 10.1021/acs.jpca.7b00058.

Comparison of B97-D and other dispersion corrected methods, the comparison of CPU time between CCSD(T), MP2 and seven DFT, the differences of average adjacent O−O distance between MP2/aug-cc-pVDZ and MP2/aug-cc-pVTZ results, the interaction energies of CCSD(T) and MP2 at CBS limit, the harmonic and anharmonic frequencies, and the Cartesian coordinates of the isomers (PDF)

■ AUTHOR INFORMATION

Corresponding Author

*(Y.S.) E-mail, su.yan@dlut.edu.cn.

ORCID

Yan Su: 0000-0001-5669-9015

Jijun Zhao: 0000-0002-3263-7159

Notes

The authors declare no competing financial interest.

■ ACKNOWLEDGMENTS

This work was supported by the National Natural Science Foundation of China (11404051, 11674046, 11604039), the Fundamental Research Funds for the Central Universities of China (DUT16LAB01, DUT15RC(3)099) and the Supercomputing Center of Dalian University of Technology.

■ REFERENCES

(1) Finney, J. L. Water? What's so special about it? *Philos. Trans. R. Soc., B* **2004**, *359*, 1145−1165.

(2) Kim, K.; Jordan, K. D.; Zwier, T. S. Low-energy structures and vibrational frequencies of the water hexamer: Comparison with benzene-$(H_2O)_6$. *J. Am. Chem. Soc.* **1994**, *116*, 11568−11569.

(3) Aloisio, S.; Francisco, J. S. Radical-water complexes in Earth's atmosphere. *Acc. Chem. Res.* **2000**, *33*, 825−830.

(4) Maheshwary, S.; Patel, N.; Sathyamurthy, N.; Kulkarni, A. D.; Gadre, S. R. Structure and stability of water clusters $(H_2O)_n$, n = 8−20: An ab initio investigation. *J. Phys. Chem. A* **2001**, *105*, 10525−10537.

(5) Robertson, W. H.; Diken, E. G.; Johnson, M. A. Snapshots of water at work. *Science* **2003**, *301*, 320−321.

(6) Miyazaki, M.; Fujii, A.; Ebata, T.; Mikami, N. Infrared spectroscopic evidence for protonated water clusters forming nanoscale cages. *Science* **2004**, *304*, 1134−1137.

(7) Shin, J.-W.; Hammer, N. I.; Diken, E. G.; Johnson, M. A.; Walters, R. S.; Jaeger, T. D.; Duncan, M. A.; Christie, R. A.; Jordan, K. D. Infrared signature of structures associated with the $H^+(H_2O)_n$ (n = 6 to 27) clusters. *Science* **2004**, *304*, 1137−1140.

(8) Beyer, M. K. Hydrated metal ions in the gas phase. *Mass Spectrom. Rev.* **2007**, *26*, 517−541.

(9) Ma, L.; Majer, K.; Chirot, F.; von Issendorff, B. Low temperature photoelectron spectra of water cluster anions. *J. Chem. Phys.* **2009**, *131*, 144303.

(10) Jungwirth, P. Spiers Memorial Lecture Ions at aqueous interfaces. *Faraday Discuss.* **2009**, *141*, 9−30.

(11) Hermansson, K.; Bopp, P. A.; Spångberg, D.; Pejov, L.; Bakó, I.; Mitev, P. D. The vibrating hydroxide ion in water. *Chem. Phys. Lett.* **2011**, *514*, 1−15.

(12) Meot-Ner (Mautner), M. Update 1 of: Strong ionic hydrogen bonds. *Chem. Rev.* **2012**, *112*, PR22−PR103.

(13) Gadre, S. R.; Yeole, S. D.; Sahu, N. Quantum chemical investigations on molecular clusters. *Chem. Rev.* **2014**, *114*, 12132−12173.

(14) Baker, E. N.; Hubbard, R. E. Hydrogen bonding in globular proteins. *Prog. Biophys. Mol. Biol.* **1984**, *44*, 97−179.

(15) Robinson, G. W.; Thistlethwaite, P. J.; Lee, J. Molecular aspects of ionic hydration reactions. *J. Phys. Chem.* **1986**, *90*, 4224−4233.

(16) Ludwig, R. Water: From clusters to the bulk. *Angew. Chem., Int. Ed.* **2001**, *40*, 1808−1827.

(17) Vendrell, O.; Meyer, H.-D. A proton between two waters: insight from full-dimensional quantum-dynamics simulations of the $[H_2O\text{-}H\text{-}OH_2]^+$cluster. *Phys. Chem. Chem. Phys.* **2008**, *10*, 4692−4703.

(18) Good, A.; Durden, D. A.; Kebarle, P. Ion−molecule reactions in pure nitrogen and nitrogen containing traces of water at total pressures 0.5−4 Torr. Kinetics of clustering reactions forming $H^+(H_2O)_n$. *J. Chem. Phys.* **1970**, *52*, 212−221.

(19) Eigen, M. Proton transfer, acid-base catalysis, and enzymatic hydrolysis. Part I: ELEMENTARY PROCESSES. *Angew. Chem., Int. Ed. Engl.* **1964**, *3*, 1−19.

(20) Narcisi, R. S.; Bailey, A. D. Mass spectrometric measurements of positive ions at altitudes from 64 to 112 kilometers. *J. Geophys. Res.* **1965**, *70*, 3687−3700.

(21) Castleman, A. W.; Keesee, R. G. Ionic clusters. *Chem. Rev.* **1986**, *86*, 589−618.

(22) Garvey, J. F.; Herron, W. J.; Vaidyanathan, G. Probing the structure and reactivity of hydrogen-bonded clusters of the type $\{M\}_n\{H_2O\}H^+$, via the observation of magic numbers. *Chem. Rev.* **1994**, *94*, 1999−2014.

(23) Zundel, G.; Metzger, H. Energiebänder der tunnelnden Überschuß-Protonen in flüssigen Säuren. Eine IR-spektroskopische Untersuchung der Natur der Gruppierungen $H_5O_2^+$. *Z. Phys. Chem.* **1968**, *58*, 225−245.

(24) Yeh, L. I.; Okumura, M.; Myers, J. D.; Price, J. M.; Lee, Y. T. Vibrational spectroscopy of the hydrated hydronium cluster ions $H_3O^+\cdot(H_2O)_n$ (n = 1,2,3). *J. Chem. Phys.* **1989**, *91*, 7319−7330.

(25) Okumura, M.; Yeh, L. I.; Myers, J. D.; Lee, Y. T. Infrared spectra of the solvated hydronium ion: Vibrational predissociation spectroscopy of mass-selected $H_3O^+\cdot H_2O)_n\cdot(H2)_m$. *J. Phys. Chem.* **1990**, *94*, 3416−3427.

(26) Wang, Y.-S.; Jiang, J. C.; Cheng, C.-L.; Lin, S. H.; Lee, Y. T.; Chang, H.-C. Identifying 2- and 3-coordinated H_2O in protonated ion-water clusters by vibrational pre-dissociation spectroscopy and ab initio calculations. *J. Chem. Phys.* **1997**, *107*, 9695−9698.

(27) Asmis, K. R.; Pivonka, N. L.; Santambrogio, G.; Brümmer, M.; Kaposta, C.; Neumark, D. M.; Wöste, L. Gas-phase infrared spectrum of the protonated water dimer. *Science* **2003**, *299*, 1375−1377.

(28) Headrick, J. M.; Bopp, J. C.; Johnson, M. A. Predissociation spectroscopy of the argon-solvated $H_5O_2^+$ "zundel" cation in the 1000−1900 cm^{-1} region. *J. Chem. Phys.* **2004**, *121*, 11523−11526.

(29) Devlin, J. P.; Severson, M. W.; Mohamed, F.; Sadlej, J.; Buch, V.; Parrinello, M. Experimental and computational study of isotopic effects within the Zundel ion. *Chem. Phys. Lett.* **2005**, *408*, 439−444.

(30) Hammer, N. I.; Diken, E. G.; Roscioli, J. R.; Johnson, M. A.; Myshakin, E. M.; Jordan, K. D.; McCoy, A. B.; Huang, X.; Bowman, J. M.; Carter, S. The vibrational predissociation spectra of the $H_5O_2^+\bullet RG_n$ (RG = Ar,Ne) clusters: Correlation of the solvent perturbations in the free OH and shared proton transitions of the Zundel ion. *J. Chem. Phys.* **2005**, *122*, 244301−244301.

(31) McCunn, L. R.; Roscioli, J. R.; Johnson, M. A.; McCoy, A. B. An H/D isotopic substitution study of the $H_5O_2^+\cdot$Ar vibrational predissociation spectra: Exploring the putative role of Fermi resonances in the bridging proton fundamentals. *J. Phys. Chem. B* **2008**, *112*, 321−327.

(32) McCunn, L. R.; Roscioli, J. R.; Elliott, B. M.; Johnson, M. A.; McCoy, A. B. Why does argon bind to deuterium? Isotope effects and structures of $Ar\cdot H_5O_2^+$ complexes. *J. Phys. Chem. A* **2008**, *112*, 6074−6078.

(33) Jiang, J.-C.; Wang, Y.-S.; Chang, H.-C.; Lin, S. H.; Lee, Y. T.; Niedner-Schatteburg, G.; Chang, H.-C. Infrared spectra of

DOI: 10.1021/acs.jpca.7b00058
J. Phys. Chem. A XXXX, XXX, XXX−XXX

$H^+(H_2O)_{5-8}$ clusters: Evidence for symmetric proton hydration. *J. Am. Chem. Soc.* **2000**, *122*, 1398−1410.
(34) Headrick, J. M.; Diken, E. G.; Walters, R. S.; Hammer, N. I.; Christie, R. A.; Cui, J.; Myshakin, E. M.; Duncan, M. A.; Johnson, M. A.; Jordan, K. D. Spectral signatures of hydrated proton vibrations in water clusters. *Science* **2005**, *308*, 1765−1769.
(35) Kozack, R. E.; Jordan, P. C. Empirical models for the hydration of protons. *J. Chem. Phys.* **1992**, *96*, 3131−3136.
(36) Hodges, M. P.; Stone, A. J. Modeling small hydronium-water clusters. *J. Chem. Phys.* **1999**, *110*, 6766−6772.
(37) Hodges, M. P.; Wales, D. J. Global minima of protonated water clusters. *Chem. Phys. Lett.* **2000**, *324*, 279−288.
(38) Kuo, J.-L.; Klein, M. L. Structure of protonated water clusters: Low-energy structures and finite temperature behavior. *J. Chem. Phys.* **2005**, *122*, 024516.
(39) Vostrikov, A. A.; Drozdov, S. V.; Rudnev, V. S.; Kurkina, L. I. Molecular dynamics study of neutral and charged water clusters. *Comput. Mater. Sci.* **2006**, *35*, 254−260.
(40) Luo, Y.; Maeda, S.; Ohno, K. Quantum chemistry study of $H^+(H_2O)_8$: A global search for its isomers by the scaled hypersphere search method, and its thermal behavior. *J. Phys. Chem. A* **2007**, *111*, 10732−10737.
(41) Nguyen, Q. C.; Ong, Y.-S.; Kuo, J.-L. A hierarchical approach to study the thermal behavior of protonated water clusters $H^+(H_2O)_n$. *J. Chem. Theory Comput.* **2009**, *5*, 2629−2639.
(42) Bankura, A.; Chandra, A. A first principles theoretical study of the hydration structure and dynamics of an excess proton in water clusters of varying size and temperature. *Chem. Phys.* **2011**, *387*, 92−102.
(43) Do, H.; Besley, N. A. Structural optimization of molecular clusters with density functional theory combined with basin hopping. *J. Chem. Phys.* **2012**, *137*, 134106.
(44) Park, M.; Shin, I.; Singh, N. J.; Kim, K. S. Eigen and Zundel forms of small protonated water clusters: Structures and infrared spectra. *J. Phys. Chem. A* **2007**, *111*, 10692−10702.
(45) Yu, H.; Cui, Q. The vibrational spectra of protonated water clusters: A benchmark for self-consistent-charge density-functional tight binding. *J. Chem. Phys.* **2007**, *127*, 234504.
(46) Karthikeyan, S.; Kim, K. S. Structure, stability, thermodynamic properties, and IR spectra of the protonated water decamer $H^+(H_2O)_{10}$. *J. Phys. Chem. A* **2009**, *113*, 9237−9242.
(47) Vendrell, O.; Gatti, F.; Meyer, H.-D. Strong isotope effects in the infrared spectrum of the Zundel cation. *Angew. Chem., Int. Ed.* **2009**, *48*, 352−355.
(48) Douberly, G. E.; Walters, R. S.; Cui, J.; Jordan, K. D.; Duncan, M. A. Infrared spectroscopy of small protonated water clusters, $H^+(H_2O)_n$ (n = 2−5): Isomers, argon tagging, and deuteration. *J. Phys. Chem. A* **2010**, *114*, 4570−4579.
(49) Kaledin, M.; Wood, C. A. Ab initio studies of structural and vibrational properties of protonated water cluster $H_7O_3^+$ and its deuterium isotopologues: An application of driven molecular dynamics. *J. Chem. Theory Comput.* **2010**, *6*, 2525−2535.
(50) Heine, N.; Fagiani, M. R.; Rossi, M.; Wende, T.; Berden, G.; Blum, V.; Asmis, K. R. Isomer-selective detection of hydrogen-bond vibrations in the protonated water hexamer. *J. Am. Chem. Soc.* **2013**, *135*, 8266−8273.
(51) Torrent-Sucarrat, M.; Anglada, J. M. Anharmonicity and the Eigen-Zundel dilemma in the IR spectrum of the protonated 21 water cluster. *J. Chem. Theory Comput.* **2011**, *7*, 467−472.
(52) Sprik, M.; Hutter, J.; Parrinello, M. Abinitio molecular dynamics simulation of liquid water: Comparison of three gradient-corrected density functionals. *J. Chem. Phys.* **1996**, *105*, 1142−1152.
(53) Li, F.; Wang, L.; Zhao, J.; Xie, J.-H.; Riley, K.; Chen, Z. What is the best density functional to describe water clusters: evaluation of widely used density functionals with various basis sets for $(H_2O)_n$ (n = 1−10). *Theor. Chem. Acc.* **2011**, *130*, 341−352.
(54) Plumley, J. A.; Dannenberg, J. J. A comparison of the behavior of functional/basis set combinations for hydrogen-bonding in the water dimer with emphasis on basis set superposition error. *J. Comput. Chem.* **2011**, *32*, 1519−1527.
(55) Liu, Y.; Zhao, J.; Li, F.; Chen, Z. Appropriate description of intermolecular interactions in the methane hydrates: An assessment of DFT methods. *J. Comput. Chem.* **2013**, *34*, 121−131.
(56) Purvis, G. D.; Bartlett, R. J. A full coupled-cluster singles and doubles model: The inclusion of disconnected triples. *J. Chem. Phys.* **1982**, *76*, 1910−1918.
(57) Raghavachari, K.; Trucks, G. W.; Pople, J. A.; Head-Gordon, M. A fifth-order perturbation comparison of electron correlation theories. *Chem. Phys. Lett.* **1989**, *157*, 479−483.
(58) Watts, J. D.; Gauss, J.; Bartlett, R. J. Coupled-cluster methods with noniterative triple excitations for restricted open-shell Hartree-Fock and other general single determinant reference functions. Energies and analytical gradients. *J. Chem. Phys.* **1993**, *98*, 8718−8733.
(59) Møller, C.; Plesset, M. S. Note on an approximation treatment for many-electron systems. *Phys. Rev.* **1934**, *46*, 618−622.
(60) Frisch, M.; Trucks, G.; Schlegel, H.; Scuseria, G.; Robb, M.; Cheeseman, J.; Scalmani, G.; Barone, V.; Mennucci, B.; Petersson, G., et al. *Gaussian 09*, Revision-A.01; Gaussian Inc.: Wallingford, CT, 2009.
(61) Becke, A. D. Density-functional exchange-energy approximation with correct asymptotic behavior. *Phys. Rev. A: At., Mol., Opt. Phys.* **1988**, *38*, 3098−3100.
(62) Lee, C.; Yang, W.; Parr, R. G. Development of the Colle-Salvetti correlation-energy formula into a functional of the electron density. *Phys. Rev. B: Condens. Matter Mater. Phys.* **1988**, *37*, 785−789.
(63) Hamprecht, F. A.; Cohen, A. J.; Tozer, D. J.; Handy, N. C. Development and assessment of new exchange-correlation functionals. *J. Chem. Phys.* **1998**, *109*, 6264−6271.
(64) Dahlke, E. E.; Truhlar, D. G. Improved density functionals for water. *J. Phys. Chem. B* **2005**, *109*, 15677−15683.
(65) Becke, A. D. Density-functional thermochemistry. V. Systematic optimization of exchange-correlation functionals. *J. Chem. Phys.* **1997**, *107*, 8554−8560.
(66) Grimme, S. Semiempirical GGA-type density functional constructed with a long-range dispersion correction. *J. Comput. Chem.* **2006**, *27*, 1787−1799.
(67) Adamo, C.; Barone, V. Toward reliable density functional methods without adjustable parameters: The PBE0 model. *J. Chem. Phys.* **1999**, *110*, 6158−6170.
(68) Stephens, P. J.; Devlin, F. J.; Chabalowski, C. F.; Frisch, M. J. Ab initio calculation of vibrational absorption and circular dichroism spectra using density functional force fields. *J. Phys. Chem.* **1994**, *98*, 11623−11627.
(69) Xu, X.; Goddard, W. A. The X3LYP extended density functional for accurate descriptions of nonbond interactions, spin states, and thermochemical properties. *Proc. Natl. Acad. Sci. U. S. A.* **2004**, *101*, 2673−2677.
(70) Zhao, Y.; Schultz, N. E.; Truhlar, D. G. Design of density functionals by combining the method of constraint satisfaction with parametrization for thermochemistry, thermochemical kinetics, and noncovalent interactions. *J. Chem. Theory Comput.* **2006**, *2*, 364−382.
(71) Dunning, T. H. Gaussian basis sets for use in correlated molecular calculations. I. The atoms boron through neon and hydrogen. *J. Chem. Phys.* **1989**, *90*, 1007−1023.
(72) Kendall, R. A.; Dunning, T. H.; Harrison, R. J. Electron affinities of the first-row atoms revisited. Systematic basis sets and wave functions. *J. Chem. Phys.* **1992**, *96*, 6796−6806.
(73) Wells, B. H.; Wilson, S. van der Waals interaction potentials: Many-body basis set superposition effects. *Chem. Phys. Lett.* **1983**, *101*, 429−434.
(74) Zhong, S.; Barnes, E. C.; Petersson, G. A. Uniformly convergent n-tuple-ζ augmented polarized (nZaP) basis sets for complete basis set extrapolations. I. Self-consistent field energies. *J. Chem. Phys.* **2008**, *129*, 184116.
(75) Halkier, A.; Helgaker, T.; Jørgensen, P.; Klopper, W.; Koch, H.; Olsen, J.; Wilson, A. K. Basis-set convergence in correlated calculations on Ne, N_2, and H_2O. *Chem. Phys. Lett.* **1998**, *286*, 243−252.

DOI: 10.1021/acs.jpca.7b00058
J. Phys. Chem. A XXXX, XXX, XXX−XXX

(76) Mijoule, C.; Latajka, Z.; Borgis, D. Density functional theory applied to proton-transfer systems. A numerical test. *Chem. Phys. Lett.* **1993**, *208*, 364−368.
(77) Wei, D.; Salahub, D. R. Hydrated proton clusters and solvent effects on the proton transfer barrier: A density functional study. *J. Chem. Phys.* **1994**, *101*, 7633−7642.
(78) Losada, M.; Leutwyler, S. Water hexamer clusters: Structures, energies, and predicted mid-infrared spectra. *J. Chem. Phys.* **2002**, *117*, 2003−2016.
(79) Dyke, T. R.; Mack, K. M.; Muenter, J. S. The structure of water dimer from molecular beam electric resonance spectroscopy. *J. Chem. Phys.* **1977**, *66*, 498−510.
(80) Medvedev, M. G.; Bushmarinov, I. S.; Sun, J.; Perdew, J. P.; Lyssenko, K. A. Density functional theory is straying from the path toward the exact functional. *Science* **2017**, *355*, 49−52.
(81) Fridgen, T. D.; McMahon, T. B.; MacAleese, L.; Lemaire, J.; Maitre, P. Infrared spectrum of the protonated water dimer in the gas phase. *J. Phys. Chem. A* **2004**, *108*, 9008−9010.
(82) Zhao, J.; Shi, R.; Sai, L.; Huang, X.; Su, Y. Comprehensive genetic algorithm for ab initio global optimization of clusters. *Mol. Simul.* **2016**, *42*, 809−819.
(83) Corongiu, G.; Kelterbaum, R.; Kochanski, E. Theoretical studies of $H^+(H_2O)_5$. *J. Phys. Chem.* **1995**, *99*, 8038−8044.

DOI: 10.1021/acs.jpca.7b00058
J. Phys. Chem. A XXXX, XXX, XXX−XXX